J Nanostruct 10(3): 660-670, Summer 2020

RESEARCH PAPER

Formation of SiC Nanocrystals Prepared by Sol-gel Processing of Green Carbon Sources and DFT Calculations

Malihe Zeraati, Kazem Tahmasebi, and Ahmad Irannejad*

Department of Materials Engineering, Shahid Bahonar University of Kerman, Kerman, Iran.

ARTICLE INFO

Article History:
Received 03 April 2020
Accepted 16 June 2020
Published 01 July 2020

Keywords:
DFT
Green Synthesis
Nanopowder
Silicon Carbide

ABSTRACT

SiC nanocrystals are synthesized by sol-gel processing with tetraethoxysilane and green carbon sources (sugar, molasses, and **stevia extract)** as starting materials. The reactions of carbon precursors and silicon were investigated using density functional theory. To obtain the discrepancy between the energy levels of the interacting orbitals of precursors, molecules were optimized using B3LYP/6-31+G(d,p) method. XRD, FE-SEM, TG-DTA and FTIR analysis were implemented in order to compare the efficiency of different carbon sources. According to XRD experiments, SiC nanocrystals prepared by sugar and molasses had no contamination, while the sample prepared by stevia has impurity in the form of carbon and silica. TG-DTA results revealed that this difference is due to the fact that the carbon source in stevia did not react efficiently with silicon. Moreover, based on the DFT study and HOMO and LUMO analysis on the reactive energy of silicon and carbon precursors, it is revealed that sugar has the best reactivity among carbon sources for SiC formation.

How to cite this article
Zeraati M., Tahmasebi K., rannejadA. Formation of SiC Nanocrystals Prepared by Sol-gel Processing of Green Carbon Sources and DFT Calculations . J Nanostruct, 2020; 10(3): 660-670. DOI: 10.22052/JNS.2020.03.019

INTRODUCTION

Many methods have been developed to produce nanosized and uniformly shaped SiC powder, such as combustion synthesis [1], CVD [2], thermal evaporation [3], sol-gel carbothermal reduction [4], plasma technique [5] and microwave synthesis [6]. The comparison of different methods is reported in Table 1.

Recently, SiC nano-powder is used for its unique mechanical [16], electrical [17], optical [18], photoluminescent [19], supercapacitative [20, 21], and thermal properties [22, 23]. However, the application of SiC as a support for catalytic materials is limited by its maximum attainable surface area [24]. Consequently, there has been a lot of efforts for finding a process to produce nanosized SiC with considerable porosity and high surface area. To produce powders with smaller particle size, surfactants incorporation is required, surfactants are usually toxic and cause polluting the environment and damaging the ecosystem [25]. Most of the materials used as carbon precursors, such as resins, are expensive petrochemicals [26]. Also, among different approaches proposed for producing SiC nano-powder, the green synthesis approach might be a beneficial method [14]. This concept includes the synthesis and manipulation of nanomaterials by an efficient, environment-friendly, and safe technique that could be used for human welfare [27-29]. Moreover, it has also received merit due to its simplicity, cost-effectiveness, and easy recoverability. This method includes the adoption of nontoxic raw materials and eco-friendly reactants and solvents as well as elimination of hazardous by-products, which are the main principles of green synthesis process [28,

* *Corresponding Author Email: tahmasebi@uk.ac.ir*

Table 1. The comparison of different methods for SiC synthesis.

Ref/ Year	Precursor		Method	Temperatures (°C)	Time (h)	Size
	Silicon	Carbon				
[2]/ 2000	Silane	Acetylene	CVD	900-1250	0.4-1	0.1– 0.2 µm
[7]/ 2009	Silicon powder	Carbon black	Ball milling	1735-1760	4-14	0.5 mm
[8]/ 2009	TEOS	Pine wood	Sol-gel (green fabrication)	1600	4	100 nm
[9]/ 2010	TEOS	Phenolic resin	Sol-gel	1600	1	30-50 nm
[5]/ 2011	Silica	Pyrolytic soot Columbian soot Cancarb soot Char Graphite	Ball milling and RF plasma technique	610	1	0.32 µm 0.23 µm 0.43 µm 10-20 µm 7-10 µm
[10]/ 2012	TEOS	Phenolic resin	Sol-gel	1500	3	0.001–6 µm
[11]/ 2013	Silicon powder	Carbon blacks	Molten salt synthesis	900–1200	6	10 nm
[12]/ 2015	TEOS	Saccharose	Sol-gel (green fabrication)	1450	10	100-300 nm
[6]/ 2017	Single crystal silicon	Activated carbon	Microwave	2200–2400	30	0.1-2 µm
[13]/ 2018	Silicon powder	Coked rice husks	Ball milling (green fabrication)	1580	3	50-120 nm
[14]/ 2018	Rice husk silica	Phenolic resin	CVD (green fabrication)	1600	3	239-662 nm
[15]/ 2018	Silicon powder	Diatomite powder phenolic resin	catalytically synthesized	1400	3	30-300 nm
This study	TEOS	Sugar Molasses Stevia extract	Sol-gel (green fabrication)	800	3	42.7 nm 43.3 nm 35.5 nm

30]. Green sol-gel is one of the best methods of chemical synthesis that is environmentally friendly and can synthesize high purity nanocrystals. This method is cost-effective and has simple preparation process that leads to nanostructured and homogeneous powder [31].

One of the best candidates for the green synthesis process is the extract of plants as the natural raw material. Due to their non-toxicity and the ability to synthesize at low temperatures and relatively high purity, these sources are of great interest. Stevia is a plant from the family of sweet herbs from South America that are grown in China, Southeast Asia [32] and Iran [33]. Stevia glycosides are used for food and beverages in some countries [34-36]. This sweet substance contains different kinds of glucose, which is used to synthesize nanoparticles such as Au [33, 37], CdO [38, 39], FeO [40], ZnS [41] and Ag [42]. On the other hand, Molasses are a dark substance from sugar beet [43]. It is made in sugar beet factories and contains 50% glucose, minerals, and amino acids. It contains nutrients for the growth of yeasts, which is mainly used in the production of alcohol and animal feed [44]. It was also used as a carbon source for the synthesis of Fe-C nano-reactors [45] and the synthesis of Ag nanoparticles [46]. Accordingly, it can be used in the sol-gel process for preparing ceramic materials, due to the relatively simple procedure, low cost, good chemical uniformity and purity, and relatively low synthesis temperatures which is necessary for obtaining ultrafine powder [10, 47, 48].

The structure and reaction mechanism of a few materials have been studied based on density functional theory (DFT) [49,51]. DFT is to simplify the molecular system and perform quantum mechanical calculations using quasi-potentials for each atom in the system [52-54].

In this study, we have applied the green synthesis concept by the sol-gel process to prepare SiC nanocrystals with different green sources of carbon including, sugar, molasses and extract stevia. In this method, the lesser harmful chemical is used to produce SiC nanocrystals and finally the efficiency of these green sources for producing pure SiC is evaluated using DFT method. The reaction mechanisms and orbitals energy of the precursors of the SiC powder are analyzed via DFT method.

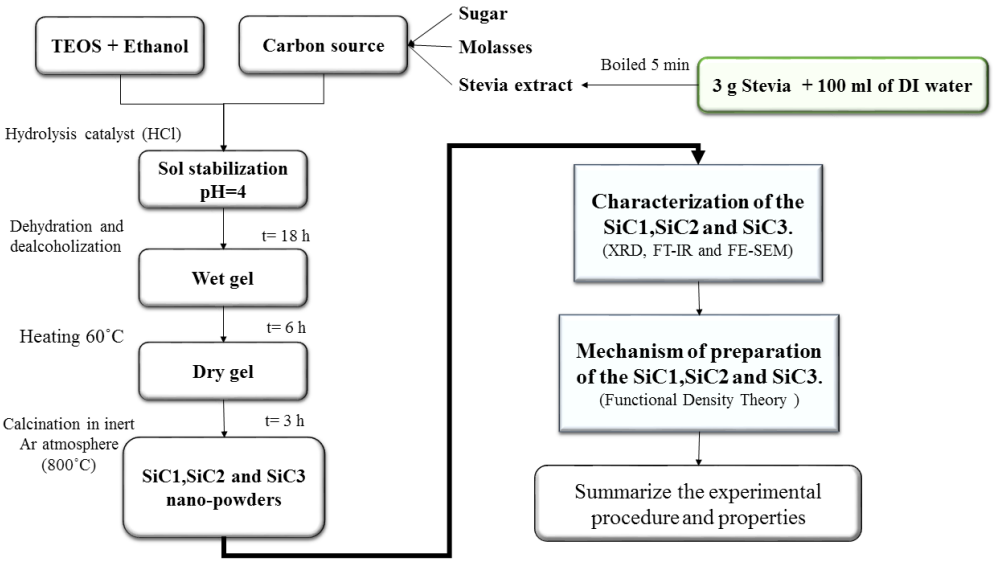

Fig. 1. The flowchart of the experimental procedure.

MATERIALS AND METHODS

Materials preparation

Tetraethyl ortho-silicate (TEOS Merck) was used as silicon source and the carbon sources were sugar, molasses and stevia**.** Also ethanol was used as solvent and hydrochloride acid (HCl Merck) as catalyst. Extract stevia was produced with thirty grams of powder of dried leaf of stevia, that was boiled in 100 ml of distilled water for 5 minutes. The details of this method are explained in the previous work [20]. Each carbon source (sugar, molasses, and stevia extract) with a constant ratio of 0.6 is mixed with other materials. In order to complete the hydrolysis reaction, the as-prepared solution was kept in an isolated place for 18 hours. Resultant gels were kept in the hot air oven for 4 hours in 60˚C to dry as shown schematically in Fig. 1. During the pyrolysis process, the samples were kept in a furnace with an argon atmosphere at 800˚ C for a time period of 3 hours.

Characterization

After sorting the samples, structural and composition analysis was performed using X-ray diffraction technique (Philips Xpert) with Cu-Kα as X-ray source. For the evaluation of agglomerates size and qualitative analysis of synthesized powders and whiskers, field-emission scanning electron microscope (FE-SEM) equipped with EDAX analyzer was used. In order to evaluate component's bond type in the gel samples, Fourier-transform infrared spectroscopy (FTIR) device was used in the range of 400–4000 cm^{-1}. Thermal analysis (TG/DTA) was also used to evaluate the nature of the reaction inside the gel samples, the rate of heating in this case, was 20 ˚C/min.

Calculations

To obtain the molecular orbital energy of silicon and carbon precursors [15], the DFT method was used. The optimization of molecule's structures by B3LYP theory using 6-31G +(d,p) bias set [55] were performed using Gaussian 09 [56]. In addition, using GaussView [57], their highest occupied molecular orbitals (HOMOs) and the lowest unauthorized molecular orbitals (LUMOs) of silicon and carbon precursors are calculated.

RESULTS AND DISCUSSION

Samples synthesized using sugar, molasses, and stevia extract, are respectively named SiC1, SiC2 and SiC3. Fig. 2 presents the FTIR spectrum for the gel prepared by the reaction of TEOS and carbon sources. The peaks at 454-463, 522-585, 947-962 and 1071-1078 cm^{-1} correspond to siloxane bonds (Si-O-Si) [7, 58]. These bonds are related to condensation reactions and hydrolysis of silicon alkoxides. The peak at 3430-3437 cm^{-1} represents OH functional groups that seem to have formed (O-H) bonds with Si atoms [59]. The peak in the range of 1642–1671 cm^{-1} belongs to doubled bonds of carbon (C=C) [9]. Moreover, 791-797

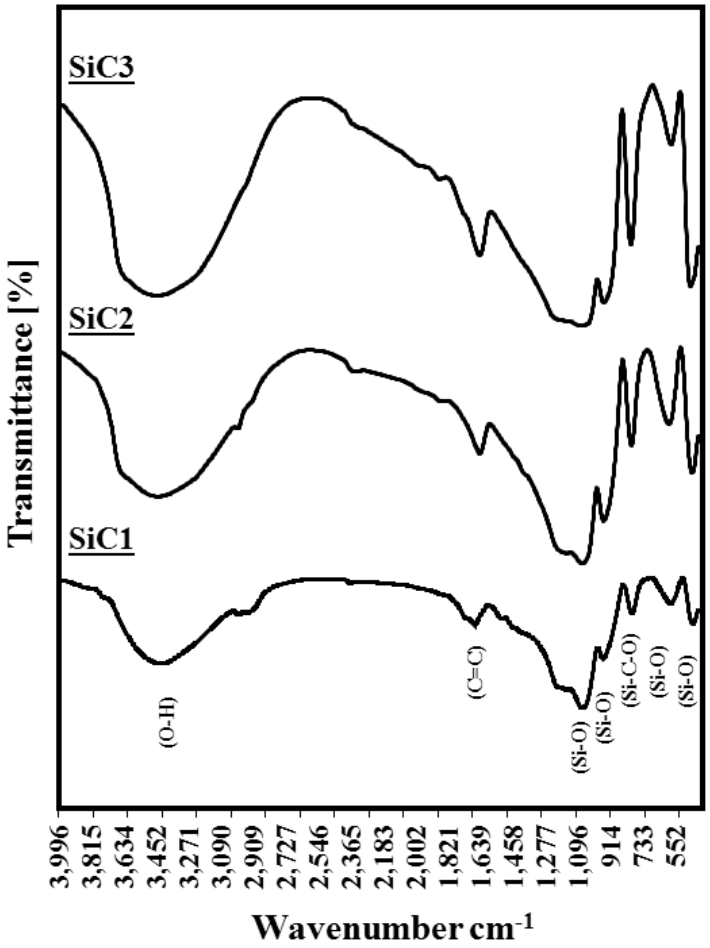

Fig. 2. FTIR spectrum for gel powders of samples.

cm^{-1} peak in this figure represents (Si-O-C) [47, 60] bonds that are originally formed between siloxane and carbon atoms from different carbon sources [61, 62]. As demonstrated in Fig. 2, the C=C peak at 1642 cm^{-1} for SiC3 sample is weaker than other two samples [61], which means lesser amount of available carbon content, and that could be the reason for the peaks of XRD patterns (Fig. 3) which shows a lot of silicon impurity in the product prepared using the gel of this sample. The lesser amount of available carbon will lead to incomplete reaction between the carbon source and silicon source in this gel. The down-fall at 791-797 cm^{-1},which is related to Si-C-O bond, is sharper in SiC2 sample as well (Fig. 2c) [47, 60], which means that SiC2 has the highest potential for SiC formation in comparison with other two carbon sources, since Si-C-O bond can easily change to Si-C bond by heating [63, 64]. This result is consistent with the XRD patterns shown in Fig. 3.

Fig. 3 shows XRD patterns, which were used to check the crystal structures of the prepared silicon carbide particles as the synthetic product. As you can see in this figure, all samples are fully crystalline which means that the pyrolysis temperature of 800 °C was high enough to generate a crystalline product. Indexed peaks in Fig. 3 illustrates the XRD analysis of SiC nano-powder as the SiC3 sample**.** The XRD peaks at 28, 47 and 71 degrees corresponding to silicon (Si) [11] and the 34, 38, 42 and 63 degrees regarding carbon (C)[15], and the peaks of SiC are at 33, 46 and 56 degrees [65, 66]. XRD results indicate that the reaction between silicon source and the carbon source is not completed in the SiC3 sample since this sample has silicon and carbon contamination.

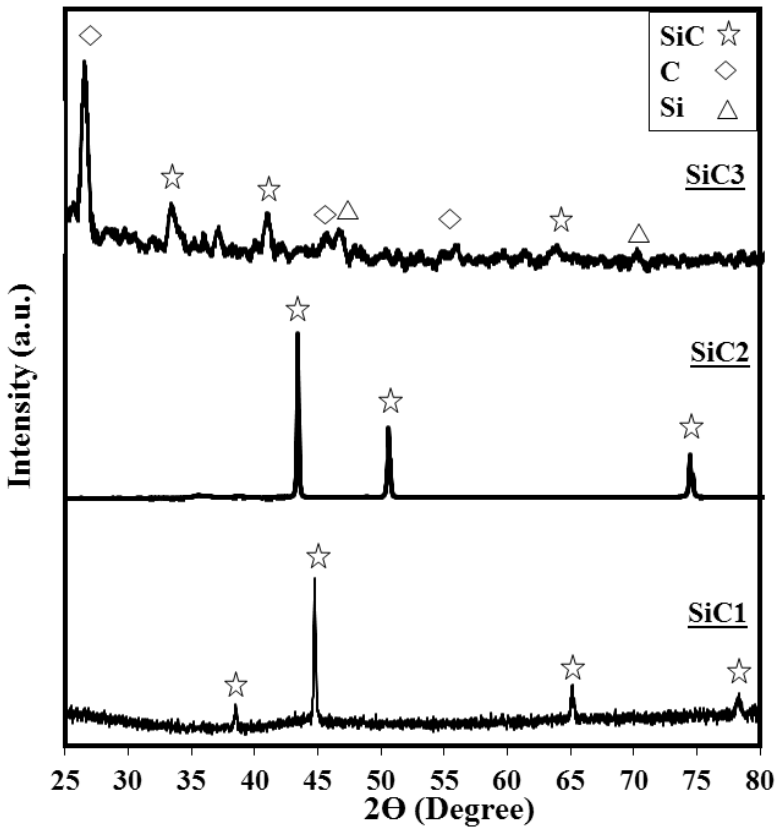

Fig. 3. XRD patterns of the SiC nano-powder samples.

Fig. 3 also illustrates the XRD patterns of SiC1 and SiC2 samples. The XRD peaks are at 38, 44, 50, 65 and 78 degrees in this figure. And as it can be seen, all of those peaks belong to silicon carbide. This points out that the samples prepared by SiC1 and SiC2 precursors have no contamination and the SiC peaks in the SiC2 sample are sharper. According to Fig. 2, the SiC1 and SiC2 have stronger doubled bonds of (C=C) and (Si-O-C) compared to SiC3. These results support the idea that the reaction between molasses and TEOS is more efficient for the production of pure crystalline SiC. Since the calcination performed in argon atmosphere, there is no evidence of SiO_2 impurity in the samples, which is due to the fact that direct carbon oxidation will not happen in the inert atmosphere [29].

The average crystallite size of the SiC nano-powder in the samples was calculated using the Scherrer equation as follows:

$$D = 0.9\lambda/(\beta \cos \theta) \quad (1)$$

Where β is FWHM (full width at half maximum) of the peaks, θ is the Bragg's angle and λ = 1.54. For crystallite size calculations, β is measured from (111) plane of SiC using the XRD pattern in Fig. 3. The calculated crystallite size of SiC, using the above equation was respectively 42.7 nm, 43.3 nm and 35.5 nm for the SiC1, SiC2, and SiC3.

Fig 4 illustrates the thermal analysis of the gel samples. From DTA analysis (Fig. 4a) it can be seen that all samples undergo similar reactions. The first endothermic peak at 160°C is due to dehydration of the sample (including the removal of the structural water) [8]. This endothermic reaction is followed by two exothermic reactions at 370 °C and 731 °C, which leads to SiC nano-powder formation (Fig. 4a) [67]. Thermogravimetric analysis of the samples (Fig. 4b) shows a secondary weight loss for the SiC3 sample, which could be due to the removal of carbon content or other volatile materials instead of the reaction of carbon with silicon. This carbon removal will reduce the amount of carbon available for SiC formation which consequently raises the amount of silicon contamination. This result confirms the

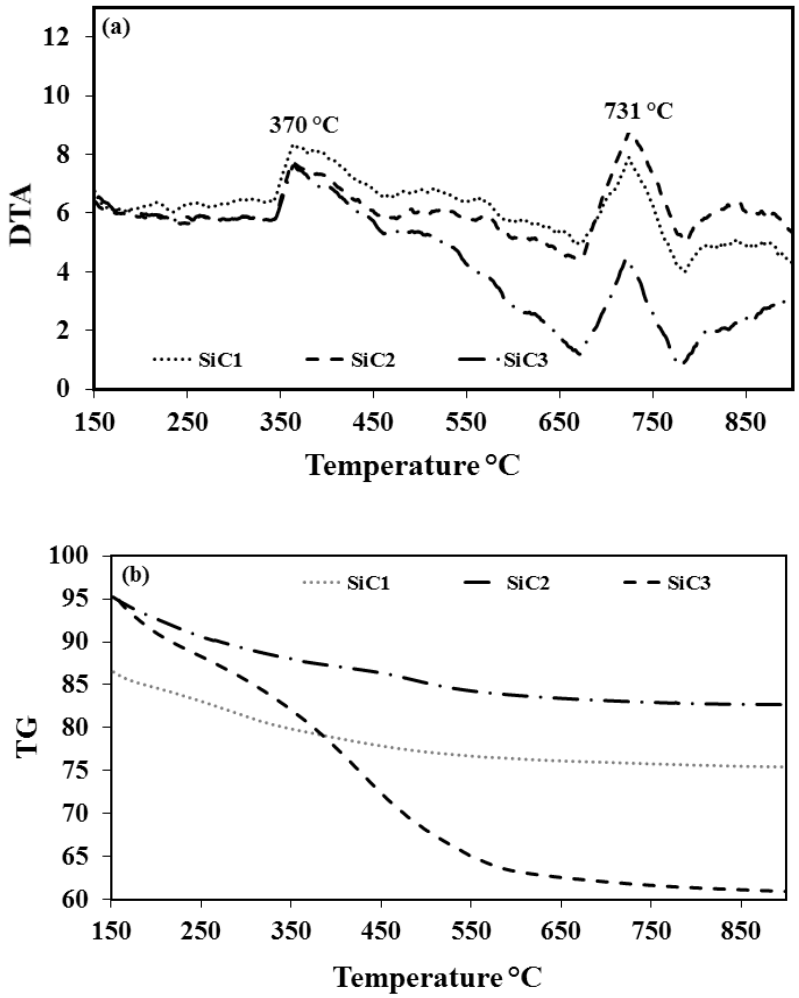

Fig. 4. Thermal analysis of the gel samples heated 20 °C/min in a nitrogen atmosphere, a) DTA analysis and, b) TG analysis of SiC precursor gel.

XRD result, which shows huge amount of silicon contamination existed in the SiC3 sample. Among three samples, the SiC2 sample has the sharpest peaks related to exothermic reactions (Fig. 4a) and also undergoes lesser weight loss due to water removal. These phenomena facilitate the SiC nano-powder formation, as it can also be seen in XRD patterns.

DFT method was used to obtain the molecular orbital energy of silicon and carbon precursors. their highest occupied molecular orbitals (HOMOs) and the lowest unauthorized molecular orbitals (LUMOs) of silicon and carbon precursors are shown in Fig. 5.

In Fig. 6 we show the reactivity of each carbon precursor, which also illustrates the energy difference of HOMO and LUMO of silicon precursor and carbon sources. As it turns out, the least energy is related to the sugar precursor, which indicates among different carbon sources, sugar reacts more efficiently with Si precursor.

There are several proposed mechanism for SiC formation using TEOS and carboneous materials [68]. Some of them assumed that the formation of SiC occurs through a direct solid state diffusion of C atoms towards the reacting interphase of SiO_2 which is formed via decomposition of TEOS. The proposed reaction is as follows:

$$SiO_2+3C=SiC+2CO \quad (1)$$

While other proposed mechanism are based on two step reaction system based on the following reactions:

$$SiO_2+C=SiO+CO \quad (2)$$

$$SiO+3CO=SiC+2CO_2 \quad (3)$$

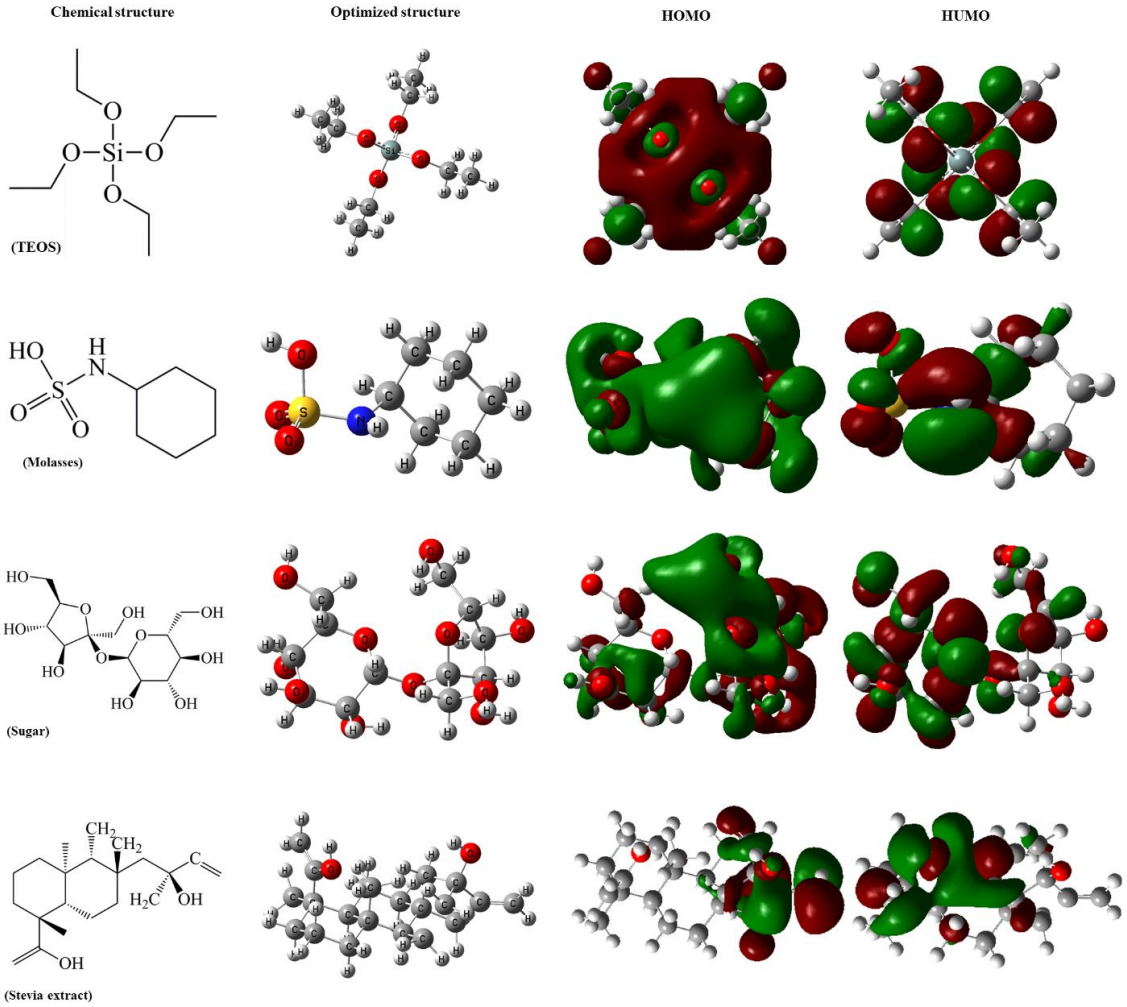

Fig. 5. Optimized structure of the silicon and carbon precursors.

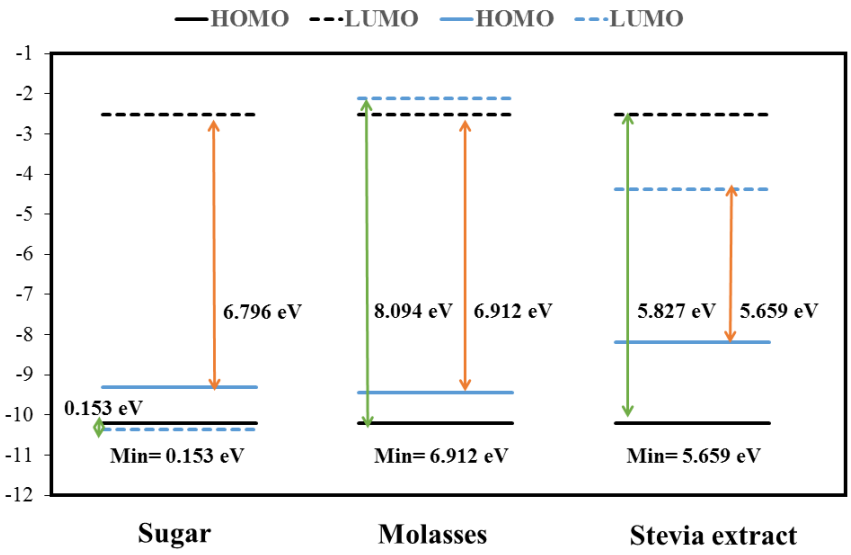

Fig. 6. The HOMO and LUMO energy levels of the silicon and carbon precursors.

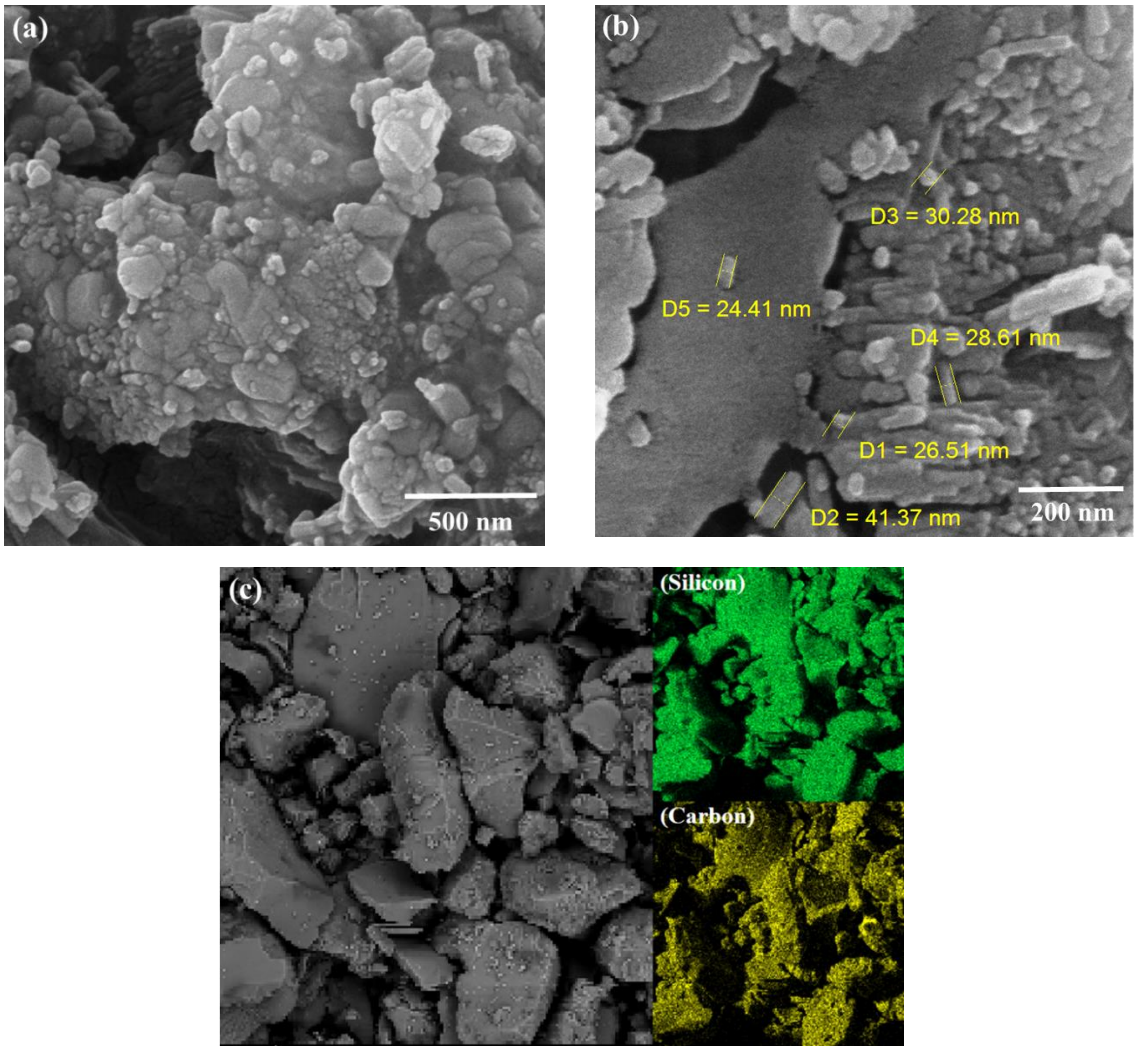

Fig. 7. a, b) FE-SEM micrographs c) MAP of elements analysis of SiC powder synthesized using molasses as a carbon source.

The work carried out on carbon/silica powder mixtures suggest that the rate of SiC formation is controlled by the rate of SiO formation. Furthermore, when the free carbon on the surface has been consumed, SiO is produced via reaction between SiO_2 and SiC as follows:

$$2SiO_2 + SiC = 3SiO + CO \quad (4)$$

When dealing with carbon and silica powders, at elevated temperatures, at the interface of C/SiO_2, a SiC layer is produced, so the silicon monoxide cannot be produced by reaction (2) anymore. The binary interface of C/SiO_2 is converted into the ternary interface of C/SiC/SiO_2, and the silicon monoxide is produced by reaction (4), and this will slow down the rate of SiC formation.

However in the case of this study carbon and silica powders are not starting materials. Instead of that a homogenous gel like mixture of carboneous material and TEOS is used, and this will lead to closest possible distance between carbon and silicon, so there is no need for carbon diffusion and that's why the reaction completes at lower temperatures in a short period of time.

The best results are obtained from sugar precursors, so FE-SEM and MAP element analysis were carried out for this sample. Fig. 7 shows the FE-SEM image of the SiC1 sample. Based on these Figs, powder prepared by this method has irregular morphology. As it can be seen from MAP elemental analysis (Fig. 7 c), SiC is formed in the entire sample surface and there are no other

impurities. The size of the agglomerates is quite larger than the size of the nano-powder measured by XRD analysis. As it is expected and reported elsewhere [69, 70], it is due to the fact that XRD measures the crystallite size but SEM shows the agglomerate size. However, the resultant powder is brittle and could be easily crushed to fine particles by simple grinding. This easy crushing capability is due to low synthesis temperature of 800°C, and in comparison with the work of Wang et al. [28], and Nersisyan et al. [2], who used 1250°C to 2300°C for synthesis, it is reasonable to expect a spongier product, since higher synthesis temperature causes strong bonding between agglomerates.

CONCLUSIONS

This study shows that SiC nano-powder could be synthesized by the sol-gel process at a relatively low temperature with easily available chemicals and green carbon sources. Among carbon sources, sugar seems to be the best candidate, as it efficiently reacts with TEOS to produce nano-powder and pure SiC nano-powder. On the other hand, stevia did not react well with TEOS due to large amount of carbon source or other volatile material that had been removed from the sample before SiC formation reaction. This result is also supported by XRD results that show contamination exists in SiC nano-powder produced by SiC3. Comparing the XRD results with Thermal analysis (TG/DTA) and FTIR analysis also proves the efficiency of molasses as a green carbon source for the production SiC nano-powder. The SiC nano-powder formation mechanism was investigated using the DFT method. As HOMO and LUMO analysis shown in this research, sugar has better reactivity with Si precursor for the formation of SiC.

CONFLICT OF INTEREST

The authors declare that there are no conflicts of interest regarding the publication of this manuscript.

REFERENCES

1. Li Z, Zhang J, Meng A, Guo J. Large-Area Highly-Oriented SiC Nanowire Arrays: Synthesis, Raman, and Photoluminescence Properties. The Journal of Physical Chemistry B. 2006;110(45):22382-6.
2. Kavecký Š, Janeková B, Madejová J, Šajgalík P. Silicon carbide powder synthesis by chemical vapour deposition from silane/acetylene reaction system. Journal of the European Ceramic Society. 2000;20(12):1939-46.
3. Seog IS, Kim CH. Preparation of monodispersed spherical silicon carbide by the sol-gel method. Journal of Materials Science. 1993;28(12):3277-82.
4. Borsella E, Botti S, Martelli S. Nano-Powders From Gas-Phase Laser Driven Reactions: Characteristics and Applications. Materials Science Forum. 1996;235-238:261-6.
5. Károly Z, Mohai I, Klébert S, Keszler A, Sajó IE, Szépvölgyi J. Synthesis of SiC powder by RF plasma technique. Powder Technology. 2011;214(3):300-5.
6. Zhao M, Johnson M, He W, Li G, Zhao C, Huang J, et al. Transformation of waste crystalline silicon into submicro β-SiC by multimode microwave sintering with low carbon emissions. Powder Technology. 2017;322:290-5.
7. Yang Y, Lin Z-M, Li J-T. Synthesis of SiC by silicon and carbon combustion in air. Journal of the European Ceramic Society. 2009;29(1):175-80.
8. Locs J, Berzina-Cimdina L, Zhurinsh A, Loca D. Optimized vacuum/pressure sol impregnation processing of wood for the synthesis of porous, biomorphic SiC ceramics. Journal of the European Ceramic Society. 2009;29(8):1513-9.
9. Najafi A, Golestani-Fard F, Rezaie HR, Ehsani N. Effect of APC addition on stability of nanosize precursors in sol–gel processing of SiC nanopowder. Journal of Alloys and Compounds. 2010;505(2):692-7.
10. Najafi A, Fard FG, Rezaie HR, Ehsani N. Synthesis and characterization of SiC nano powder with low residual carbon processed by sol–gel method. Powder Technology. 2012;219:202-10.
11. Ye J, Zhang S, Lee WE. Molten salt synthesis and characterization of SiC coated carbon black particles for refractory castable applications. Journal of the European Ceramic Society. 2013;33(10):2023-9.
12. Omidi Z, Ghasemi A, Bakhshi SR. Synthesis and characterization of SiC ultrafine particles by means of sol-gel and carbothermal reduction methods. Ceramics International. 2015;41(4):5779-84.
13. Li W, Guo H. A novel and green fabrication of 3C-SiC nanowires from coked rice husk-silicon mixture and their photoluminescence property. Materials Letters. 2018;215:75-8.
14. Li W, Huang Q, Guo H, Hou Y. Green synthesis and photoluminescence property of β-SiC nanowires from rice husk silica and phenolic resin. Ceramics International. 2018;44(4):4500-3.
15. Wang J, Zhang Y, Zhang H, Han L, Bi Y, Wang H, et al. Low-temperature catalytic synthesis of SiC nanopowder from liquid phenolic resin and diatomite. Advances in Applied Ceramics. 2017;117(3):147-54.
16. Zayachuk Y, Karamched P, Deck C, Hosemann P, Armstrong DEJ. Linking microstructure and local mechanical properties in SiC-SiC fiber composite using micromechanical testing. Acta Materialia. 2019;168:178-89.
17. Chen S, Kou Z, Li Y, Wang Z, Zhang Y, Yuan L, et al. Progress to electrical properties of diamond-SiC composites under high pressure and high temperature. Diamond and Related Materials. 2019;94:203-8.
18. Lu X, Zhao T, Lei Q, Yan X, Ren J, La P. Effects of co-doping on electronic structure and optical properties of 3C-SiC from first-principles method. Computational Materials Science. 2019;170:109172.
19. Formation of nitrogen-vacancy centers in 4H-SiC and their near infrared photoluminescence properties. J Appl Phys. 2019;126(8):083105.
20. Zeraati M, Tahmasebi K. Supercapacitor behavior of SiC coated copper hydroxide and copper sulfide nano-wires.

Journal of Alloys and Compounds. 2019;786:798-807.
21. Li W, Liu Q, Fang Z, Wang L, Chen S, Gao F, et al. On-Chip Supercapacitors: All-Solid-State On-Chip Supercapacitors Based on Free-Standing 4 H -SiC Nanowire Arrays (Adv. Energy Mater. 17/2019). Advanced Energy Materials. 2019;9(17):1970060.
22. Dai H, Wong EW, Lu YZ, Fan S, Lieber CM. Synthesis and characterization of carbide nanorods. Nature. 1995;375(6534):769-72.
23. Lanfant B, Leconte Y, Debski N, Bonnefont G, Pinault M, Mayne-L'Hermite M, et al. Mechanical, thermal and electrical properties of nanostructured CNTs/SiC composites. Ceramics International. 2019;45(2):2566-75.
24. Wei Q, Yang G, Yoneyama Y, Vitidsant T, Tsubaki N. Designing a novel Ni–Al2O3–SiC catalyst with a stereo structure for the combined methane conversion process to effectively produce syngas. Catalysis Today. 2016;265:36-44.
25. Wen L, Ma Y, Dai B, Zhou Y, Liu J, Pei C. Preparation and dielectric properties of SiC nanowires self-sacrificially templated by carbonated bacterial cellulose. Materials Research Bulletin. 2013;48(2):687-90.
26. Khomand E, Afsharpour M. Green synthesis of nanostructured SiCs by using natural biopolymers (guar, tragacanth, Arabic, and xanthan gums) for oxidative desulfurization of model fuel. International Journal of Environmental Science and Technology. 2018;16(5):2359-72.
27. Kundu M, Karunakaran G, Kuznetsov D. Green synthesis of NiO nanostructured materials using Hydrangea paniculata flower extracts and their efficient application as supercapacitor electrodes. Powder Technology. 2017;311:132-6.
28. Wang T, Liu S. Green synthesis and photoluminescence property of AlOOH nanoflakes. Powder Technology. 2016;294:280-3.
29. Karunakaran G, Jagathambal M, Venkatesh M, Suresh Kumar G, Kolesnikov E, Dmitry A, et al. Hydrangea paniculata flower extract-mediated green synthesis of MgNPs and AgNPs for health care applications. Powder Technology. 2017;305:488-94.
30. Zhang YC, Wu X, Ya Hu X, Guo R. Low-temperature synthesis of nanocrystalline ZnO by thermal decomposition of a "green" single-source inorganic precursor in air. Journal of Crystal Growth. 2005;280(1-2):250-4.
31. Foo YT, Foo LT, Shahcheragh L, Horri BA, Salamatinia B. Green Synthesis and Characterization of High-Purity Monodispersed Cupric Oxide (CuO) Nanopowder. Key Engineering Materials. 2019;801:351-6.
32. Koyama E, Sakai N, Ohori Y, Kitazawa K, Izawa O, Kakegawa K, et al. Absorption and metabolism of glycosidic sweeteners of stevia mixture and their aglycone, steviol, in rats and humans. Food and Chemical Toxicology. 2003;41(6):875-83.
33. Sadeghi B, Mohammadzadeh M, Babakhani B. Green synthesis of gold nanoparticles using Stevia rebaudiana leaf extracts: Characterization and their stability. Journal of Photochemistry and Photobiology B: Biology. 2015;148:101-6.
34. Kim NC, Kinghorn AD. Highly sweet compounds of plant origin. Archives of Pharmacal Research. 2002;25(6):725-46.
35. Singh G, Singh G, Singh P, Parmar R, Paul N, Vashist R, et al. Molecular dissection of transcriptional reprogramming of steviol glycosides synthesis in leaf tissue during developmental phase transitions in Stevia rebaudiana Bert. Scientific Reports. 2017;7(1).
36. Harismah K, Mirzaei M, Fuadi AM. Stevia rebaudiana in Food and Beverage Applications and Its Potential Antioxidant and Antidiabetic: Mini Review. Advanced Science Letters. 2018;24(12):9133-7.
37. Engelbrekt C, Sørensen KH, Zhang J, Welinder AC, Jensen PS, Ulstrup J. Green synthesis of gold nanoparticles with starch–glucose and application in bioelectrochemistry. Journal of Materials Chemistry. 2009;19(42):7839.
38. Karthik K, Dhanuskodi S, Gobinath C, Prabukumar S, Sivaramakrishnan S. Multifunctional properties of CdO nanostructures Synthesised through microwave assisted hydrothermal method. Materials Research Innovations. 2018;23(5):310-8.
39. Karthik K, Dhanuskodi S, Gobinath C, Prabukumar S, Sivaramakrishnan S. Andrographis paniculata extract mediated green synthesis of CdO nanoparticles and its electrochemical and antibacterial studies. Journal of Materials Science: Materials in Electronics. 2017;28(11):7991-8001.
40. Khatami M, Alijani HQ, Fakheri B, Mobasseri MM, Heydarpour M, Farahani ZK, et al. Super-paramagnetic iron oxide nanoparticles (SPIONs): Greener synthesis using Stevia plant and evaluation of its antioxidant properties. Journal of Cleaner Production. 2019;208:1171-7.
41. Alijani HQ, Pourseyedi S, Torkzadeh Mahani M, Khatami M. Green synthesis of zinc sulfide (ZnS) nanoparticles using Stevia rebaudiana Bertoni and evaluation of its cytotoxic properties. Journal of Molecular Structure. 2019;1175:214-8.
42. Laguta I, Stavinskaya O, Kazakova O, Fesenko T, Brychka S. Green synthesis of silver nanoparticles using Stevia leaves extracts. Applied Nanoscience. 2018;9(5):755-65.
43. Nakane K, Ogihara T, Ogata N, Kurokawa Y. Entrap-immobilization of invertase on composite gel fiber of cellulose acetate and zirconium alkoxide by sol-gel process. Journal of Applied Polymer Science. 2001;81(9):2084-8.
44. Küçükkömürler S. Vitaminler. Beslenme ve Sağlık: Pegem Akademi Yayıncılık; 2019. p. 111-24.
45. Wróblewska A, Makuch E, Młodzik J, Michalkiewicz B. Fe-carbon nanoreactors obtained from molasses as efficient catalysts for limonene oxidation. nano Online: De Gruyter; 2018.
46. Hemmati S, Retzlaff-Roberts E, Scott C, Harris MT. Artificial Sweeteners and Sugar Ingredients as Reducing Agent for Green Synthesis of Silver Nanoparticles. Journal of Nanomaterials. 2019;2019:1-16.
47. Qian J-M, Wang J-P, Qiao G-J, Jin Z-H. Preparation of porous SiC ceramic with a woodlike microstructure by sol-gel and carbothermal reduction processing. Journal of the European Ceramic Society. 2004;24(10-11):3251-9.
48. Xing X, Deng J, Chen J, Liu G. Phase evolution of barium titanate from alkoxide gel-derived precursor. Journal of Alloys and Compounds. 2004;384(1-2):312-7.
49. Cai W, Bulatov VV, Chang J, Li J, Yip S. Anisotropic Elastic Interactions of a Periodic Dislocation Array. Physical Review Letters. 2001;86(25):5727-30.
50. Mirzaei M, Mirzaei M. The B-doped SiC nanotubes: A computational study. Journal of Molecular Structure: THEOCHEM. 2010;953(1-3):134-8.
51. Kouchaki A, Gülseren O, Hadipour N, Mirzaei M. Relaxations of fluorouracil tautomers by decorations of fullerene-like SiCs: DFT studies. Physics Letters A.

2016;380(25-26):2160-6.
52. Shakiba M, Khayati GR, Zeraati M. State-of-the-art predictive modeling of hydroxyapatite nanocrystallite size: a hybrid density functional theory and artificial neural networks. Journal of Sol-Gel Science and Technology. 2019;92(3):641-51.
53. Mirzaei M. Density Functional Study of Defects in Boron Nitride Nanotubes. Zeitschrift für Physikalische Chemie. 2009;223(7):815-23.
54. Mirzaei M, Mirzaei M. The C-doped AlP nanotubes: A computational study. Solid State Sciences. 2011;13(1):244-50.
55. Bouzzine SM, Bouzakraoui S, Bouachrine M, Hamidi M. Density functional theory (B3LYP/6-31G*) study of oligothiophenes in their aromatic and polaronic states. Journal of Molecular Structure: THEOCHEM. 2005;726(1-3):271-6.
56. Frisch M, Gaussian 09, Revision A. 01, Gaussian Inc. Wallingford CT 2009 (2009). https://doi.org/10.1145/1599301.1599384
57. Dennington R, Keith T, Millam J, GaussView, version 5, Semichem Inc.: Shawnee Mission, KS (2009). https://doi.org/10.21236/ada330871
58. Baitalik S, Kayal N. Processing and properties of cordierite-silica bonded porous SiC ceramics. Ceramics International. 2017;43(17):14683-92.
59. Singh BP, Jena J, Besra L, Bhattacharjee S. Dispersion of nano-silicon carbide (SiC) powder in aqueous suspensions. Journal of Nanoparticle Research. 2006;9(5):797-806.
60. Zhang J, Liu X, Jia Q, Huang J, Zhang S. Novel synthesis of ultra-long single crystalline β-SiC nanofibers with strong blue/green luminescent properties. Ceramics International. 2016;42(3):4600-6.
61. Du H, Ren Z, Xu Y. Microwave-induced shape-memory poly(vinyl alcohol)/poly(acrylic acid) interpenetrating polymer networks chemically linked to SiC nanoparticles. Iranian Polymer Journal. 2018;27(9):621-8.
62. Chen H, Jiang J, Zhao H. Synthesis of highly dispersed silicon carbide powders by a solvothermal-assisted sol–gel process. Applied Physics A. 2018;124(7).
63. Liu Y, Fu Q, Lin H, Wang B, Li L. Synthesis and characterisation of self-assembled SiC nanowires and nanoribbons by using sol–gel carbothermal reduction. Advances in Applied Ceramics. 2017;117(1):23-9.
64. Yang W, Miao H, Xie Z, Zhang L, An L. Synthesis of silicon carbide nanorods by catalyst-assisted pyrolysis of polymeric precursor. Chemical Physics Letters. 2004;383(5-6):441-4.
65. Ryu Y, Tak Y, Yong K. Direct growth of core–shell SiC–SiO2nanowires and field emission characteristics. Nanotechnology. 2005;16(7):S370-S4.
66. Konno H, Sato Sy, Kimura Ki, Habazaki H. Synthesis and characterization of balloons and porous blocks of β-SiC using silicone and urethane foam. Journal of the European Ceramic Society. 2007;27(1):405-12.
67. Vix-Guterl C, Alix I, Ehrburger P. Synthesis of tubular silicon carbide (SiC) from a carbon–silica material by using a reactive replica technique: mechanism of formation of SiC. Acta Materialia. 2004;52(6):1639-51.
68. Tahmasebi K, Maleki Shahraki M, Ebadzadeh T. Effect of microwave sintering on the microstructure and electrical properties of low-voltage ZnO varistors. Materials and Manufacturing Processes. 2017;33(8):817-21.
69. Tahmasebi K, Paydar MH. The effect of starch addition on solution combustion synthesis of Al2O3–ZrO2 nanocomposite powder using urea as fuel. Materials Chemistry and Physics. 2008;109(1):156-63.